RADIAL OUTPUT SPACE MAPPING FOR ELETROMECHANICAL SYSTEMS DESIGN

Maya HAGE HASSAN*, Ghislain REMY*, Guillaume KREBS* and Claude MARCHAND*

*Laboratoire de Génie Electrique de Paris (LGEP) / SPEE-Labs, CNRS UMR 8507;
SUPELEC; Université Pierre et Marie Curie P6; Université Paris-Sud;
11 rue Joliot Curie, Plateau de Moulon, 91192 Gif sur Yvette CEDEX, FRANCE
E-mail: Maya.Hage-Hassan@lgep.supelec.fr

Abstract. This paper describes a multilevel Output Space Mapping (OSM) optimization technique based on Radial Basis Function (RBF) surrogate modeling. Initially, adaptive OSM through RBF surrogate modeling on a predetermined region of interest has been applied as an auxiliary mapping in order to improve the Input Space Mapping method, when dealing with non-linear or large misalignmentsbetween the response spaces of coarse and fine models. We propose using the Radial Output Space Mapping (ROSM) for the optimization of an axial flux machine without prior use of Input Space Mapping and through a progressive construction of the region of interest by means of iterative determination of the base set. Finally, the proposed ROSM is compared with the conventional OSM technique.

Keywords: Electromagnetic, multilevel optimization, space mapping, surrogate modeling.

INTRODUCTION

Achieving an optimal design in engineering applications, in terms of design specifications, is often a compromise between final solution accuracy and fast computation/simulation time. The first constraint is due to the use of an expensive, accurate model, the fine model, while the second is based on the evaluation of a faster but less accurate model, denoted as coarse model. The Space Mapping (SM) technique [1][2],conceived by Bandler in 1994, allows engineers to exploit optimization on a fine model in order to reach certain exactness on the final design without being prohibited by calculation time.

SM has been widely used as an optimization technique of microwave devices [1] and used for electromagnetic systems starting by [3], to perform optimization on an Interior Permanent Magnet (IPM) motor. Later varieties of SM techniques were applied to the optimization of a safety isolating transformer [4]. Since its conception, several approaches aiming to elaborate this technique have appeared, all attempting to improve the Parameter Extraction step, the key to establishing the mapping between the two model spaces.

Other improvements such as Aggressive Space Mapping and Trust Region Aggressive Space Mapping eliminate simulation overhead required while using the Parameter Extraction on the fine model space, through the introduction of a quasi-Newton step in the fine space exploiting each fine model iterate as soon as it is available.

In 2001, a variant of the Space Mapping technique, the Output Space Mapping (OSM) was first introduced in [2] as auxiliary mapping, to improve the performance of the Input Space Mapping algorithm. It aims to reduce misalignment between the fine and coarse models by mapping the response of the coarse model at point x_c^* to the response of the fine model at the same point. Output Space Mapping has been used in the Electromechanics domain without a prior introduction of Input Space Mapping. For example, it was adopted in the optimization of an internal permanent magnet synchronous machine [5] using two models built on a finite element analysis with different accuracy, and was also combined in a three level Output Mapping using three different accuracy level models [6][7].

Output standalone correction can be seen as a shifting of coarse model responses at each iteration independently. Therefore, for a large discrepancy between the response spaces, the correction strategy has to be reviewed for a refined correction. In this paper an output correction strategy based on Radial Basis surrogate modeling is proposed to model the error between the two models.

Through the following paragraphs, we will discuss further the OSM technique along with ROSM and a comparison between both techniques is carried out through the optimization of an Axial Flux Machine.

OUTPUT SPACE MAPPING APPROACHES

Output Space Mapping

We define the optimization problem that is to be solved on fine models as finding the fine models optimizer x_f^* that minimizes distance between m fine model outputs f_m, and corresponding m design specifications Y_m.

(1)
$$x_f^* = \arg\min_{x \in X} \| f_m(x) - Y_m \|_2^2$$

Through the introduction of the Output Space Mapping technique, the optimization problem is to be reformulated on a surrogate model (*S*). We denote by a surrogate model, the corrected coarse model (*C*), which is trained through the optimization process to fit data derived of the evaluation of the fine model. The coarse model is corrected by use of what is called a mapping output denoted as the surface in [8], and can be expressed as a local multiplicative correction coefficient (θ) that is established by minimizing the residual between the responses of the two models spaces per iteration. At i^{th} iteration it is given by:

(2) $$x_s^* = \arg\min_{x \in X} \left\| S_m^i(x) - Y_m \right\|_2^2,\ S_j^i = \theta_j^i . C_j^i(x) \text{ with } \theta_j^i = \frac{f_j^i(x)}{C_j^i(x)},\ 1 \le j \le m$$

Radial Output Space Mapping

Local model correction can be seen as a shifting of coarse model responses at each iteration independently [9], the correction strategy has to be reviewed for a refined surrogate model accuracy, in case of a non-linear or large misalignment between the response spaces (case of a poor coarse model generating very low fidelity outputs with respect to the fine ones). Using the surface concept to approach Surrogate Space Mapping based models implies the search for direct approximation methods that can be used to smoothen generated fine model data. Familiar approximation methods include polynomial modeling, response surfaces [10], radial basis functions [11] via neural nets, and kriging, [12] [13], [14]. It is worth mentioning the clear distinction between the Space Mapping approach which uses an existing physical model capable of simulating the system over a wide range of parameter values and optimization using surrogate models establishing a local approximation of fine model responses using a set of fine model simulations.

Thus, through the Surrogate Space Mapping approach, we will exploit efficient optimization using two modeling levels, sorted by their increasing cost and veracity: the coarse and fine models. In order to obtain sufficient accuracy on the global design solution, at the lowest possible cost, and to build a Meta fine model with increasing exactness through the optimization process.

The standard Output SM using an additive term [15] assumes that the surrogate model is built by correcting the coarse model responses with an additive term that reflects the residual error between both models, such that at the i^{th} iteration the surrogate model at j^{th} response is given by:

(3) $$S_j^i = C_j(x) + d_j^i$$

With $d_j^i = f_j^i - C_j^i$

Through the Radial Basis Functions (RBF) modeling method [16], an adaptive correction is endorsed that is dependent on the design variables. In other terms, a residual function will be built through an iterative process using the responses of both fine and coarse models. Residual function is given by *Rd*(*x*).

The attractive feature in radial basis function networks is their nonparametric regression nature [17], so that their primary use is in estimating model outputs without any a priori on estimated function nature.

The residual between the two models is built by the use of a linear combination of a Gaussian radial basis function, such that: $Rd(x) = \sum_{k=1}^{N} w_k h_k(x)$, where h_k the basis function at k^{th} the learning center:

(4) $$h_k(x) = \exp(-cr^2) \qquad r \ge 0 \qquad c > 0$$

Where $\boldsymbol{c}$ is kept fixed and equal to one and $r = \left\| x - x_k \right\|_2$. Weight factors $\boldsymbol{w_k}$ are computed so that they satisfy:

(5) $$\Phi . w = d \text{ , where } w = [w_1 \cdots w_N]^T,\ d = \begin{bmatrix} f^1 - c^1 \\ f^2 - c^2 \\ \vdots \\ f^N - c^N \end{bmatrix}$$

(6) $$\Phi_{lh} = \exp(-c \left\| x_l - x_h \right\|_2^2) \quad \text{for} \quad 0 \le l, h \le N$$

Φ is an ***N*x*N*** matrix.

Thus the Radial Surrogate model at the i^{th} iteration is given by:

(7) $$S^i(x) = C(x) + \sum_{k=1}^{i} w_k h_k(x)$$

Optimal designs issued from the surrogate model optimization will be acting as centers of our Radial Basis Function.Weight factors are iteratively computed. The algorithm considered here has the following steps:

1) Compute iteration on coarse model

$$x_c^i = \arg\min_{x \in X} \left\| C_m(x) - Y_m \right\|_2^2$$

2) Evaluate fine model on x_c^i, and stop if stopping criteria is satisfied.

3) If i=1, set $d^i = f^i(x) - C^i(x)$ as the first additive correction factor. If i>1 , compute the Radial Mapping using the sets of fine model outputs $\{ f^1(x), \ldots , f^i(x)\}$ and coarse outputs $\{C^1(x), \ldots , C^i(x)\}$, using Eqn. 5.

4) Compute the new surrogate model using Eqn. 6, set $i=i+1$, go to step 1.

OPTIMIZATION OF AN AXIAL SYNCHRONOUS MACHINE

In order to compare the discussed varieties of Output Space Mapping, we considered a constrained mono-objective optimization of an axial synchronous machine. Our aim is to find optimal physical characteristics of the machine with a view to minimize the machine's total losses and respect five non-linear constraints on the machine's Torques (T), Electromotive forces (Emf) and Current density (J). Total losses (E_{Total}) minimization is done with respect to a certain profile mission, the couples Torque-Speed issued from "Artemis road and urban cycles" Fig. 1, are chosen in order to fit the Torque-Speed characteristic of the machine,Fig. 2.

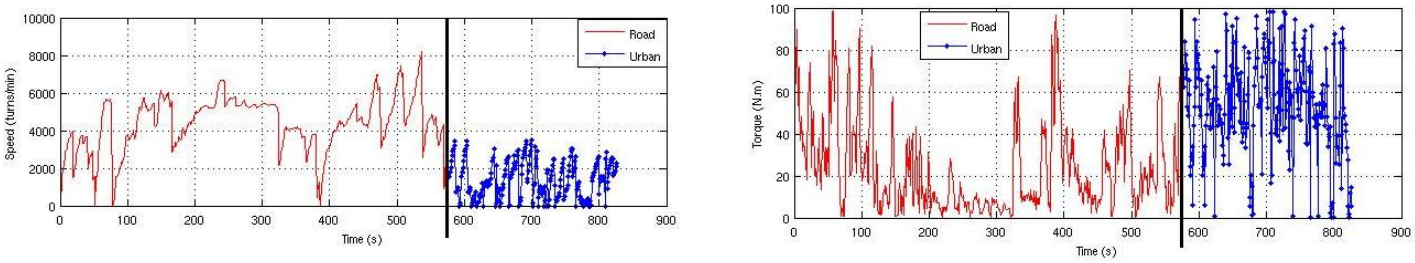

Figure 1.Artemis Cycles.

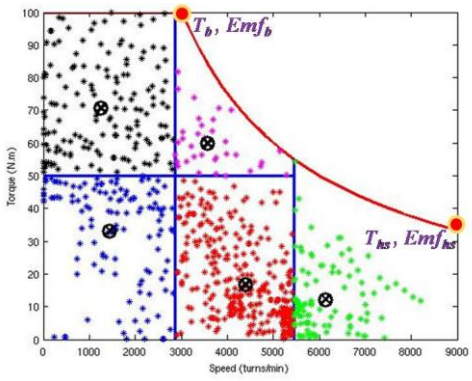

Figure 2.Torque-Speed characteristics of the machine and corresponding operating points

Optimization problem

The machine's design specifications are summarized in Table 1, and a 2D equivalent model is presented in Fig. 3.

Table 1.Model design specifications

Type	Values
Design domain	$90 \le x_1 \le 150$ (mm),$70 \le x_2 \le 110$ (mm), $5 \le x_3 \le 10$ (mm),$10 \le x_4 \le 200$ (mm), $20 \le x_5 \le 100$ (mm),$3 \le x_6 \le 50$ (turns).
Objective: total energies	$E_{Total} = E_{Iron} + E_{resistive} + E_{Inverter} + E_{Magnet}$
Nonlinear inequality constraints	$Emf_b \le 255$ (V),$Emf_{hs} \le 260$ (V), $J < 9$ (A.mm^{-2}).
Nonlinear equality constraints	$T_b = 100$ (N.m),$T_{hs} = 33.33$ (N.m).
Other Model Data	Machine $_{Length}$ = 352 (mm),Outer $_{Radius}$ = 150 (mm), Inner $_{Radius}$ = 51 (mm),N°stator $_{teeth}$ = 6, N°rotor $_{magnets}$= 8,Air$_{Gap}$ = 0.5 (mm),B_r = 1.19 (T).

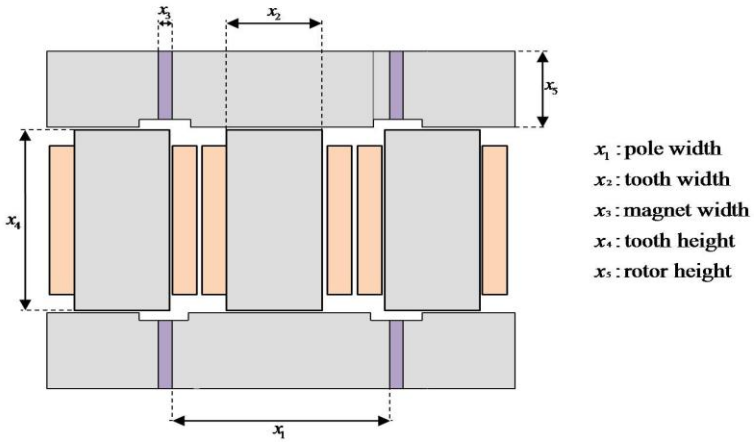

Figure 3.2D equivalent model of theAxial Flux Machine.

Fine and coarse models

The fine and coarse models are both built on a reluctance network. As for the network topology, the number of reluctances describing teeth, yokes and magnets are kept constant; as for the air gap, it is described by vertical and horizontal reluctances that depend on a discretization step *dx* that also represent the rtoric movement, such that :

(8)
$$r_h = \frac{dx}{\mu_0 a\, d} \quad , \quad r_v = \frac{a/2}{\mu_0 dx\, d}$$

Where *a* is the airgap value, *d* the machine's depth and μ_0 the relative permeability. The magnetic materials are supposed to have a linear behavior. For each displacement step, a network of reluctances is established, and a motor map in terms of flux linkages and magnetic flux density is established through the examination of all possible combinations of phase shift and magnitude of current. Through this, the average torque of each pair of phase angle and current is computed using derivatives of flux linkages and corresponding currents. The coarse model is derived from the fine model by making simplifications regarding:

a) The rotoric step dx

b) Losses in coarse model which are calculated through a barycentric method [18].

Thus, the Torque-Speed space is divided into five regions, Fig. 2, each region is represented by its barycenter and their necessary parameters required calculating equivalent losses. Five parameters are to be calculated as indicated in Table 2.

Table 2.Barycenter parameters

Expression	Parameter per barycenter i
Mean Speed and quadratic mean speed	$\langle\Omega\rangle_i$, $\langle\Omega^2\rangle_i^{1/2}$
Mean torque and quadratic mean torque	$\langle T\rangle_i$, $\langle T^2\rangle_i^{1/2}$
Number of points associated to each barycenter	N_i

The losses are calculated at each barycenter as follows:

a) The losses are calculated at each barycenter as follows:

(9)
$$(E_J)_i = N_i\, R\, I_i^2 \frac{\langle T^2\rangle_i}{\langle T\rangle_i^2},$$

Iron energetic losses per unit volume, calculated with the Bertotti formula for an unspecified periodic variation of magnetic density [19] are given by the common formula:

(10)
$$E_{iron} = \left(k_h\, f\, \Delta B_k^2 \quad + \quad k_f \frac{1}{T} \int_0^T \left(\frac{dB}{dt} \right)^2 dt \right) \Delta t$$

Where k_f and k_h are empiric coefficients characterizing iron, and can be calculated through the manufacturer's data [20], f and $1/T$ the fundamental frequency, $B(t)$ the flux density in the considered volume, Δt

the time consumed per cycle and p the number of poles. The flux density variations are considered to be sinusoidal, iron losses expression is reformulated and expressed at each barycenter as follows:

$$(E_{iron})_i = \left(k_h \frac{2p}{\pi} \langle \Omega \rangle B_{\max}^2 \quad + k_f \frac{p^2}{2} \langle \Omega^2 \rangle B_{\max}^2 \right) N_i \tag{11}$$

Similar considerations for the magnets losses, regarding the flux density are taken. Therefore the eddy-current losses per unit of magnet volume to be determined at each barycenter are expressed by [21]

$$(E_{magn})_i = \left(\frac{e_m^2}{12 \rho_m} \langle \Omega^2 \rangle B_{\max}^2 \right) N_i \tag{12}$$

Through this accuracy modification on coarse model outputs, a non-linear coarse-fine model misalignment is established, especially on a specific function, the basic torque, T_b. The determination of this output relies on the average torque map described above, therefore any alteration of the rotoric step dx will repercuss on the estimation of the basic torque at the operating point determined by the torque-speed couple (100 N.m, 314.16 rd/s), as well as on the electromotive force at basic speed. A detailed comparison between the coarse and fine models is presented in Table 3.

Table 3.Coarse and fine models specifications

Characteristic	Coarse	Fine
dx	10^{-2}	2.10^{-3}
N° Operating points	5	818
Computation time (s)	3.6	84.8

In order to simplify comparison of both models, the coarse and fine models are evaluated at X= [105, 80, 6.25, 57.5, 40, 14]. Results of these evaluation and relative errors are shown in Table 3.

Table 4.Coarse and fine models comparison table

Characteristic	Coarse	Fine	Relative error (%)
$E_{\text{resistive}}$(J)	62484	65270	4.3
E_{Iron}(J)	280990	293570	4.3
E_{Magnet}(J)	34912	37507	6.9
E_{Inverter}(J)	573800	631380	9.1
E_{Total}(J)	952186	1027727	7.4
T_b(N.m)	97.1	93.1	4.1
T_{hs}(N.m)	33.33	33.33	0
Emf_b(V)	198.53	214.1	7.5
Emf_{hs}(V)	294.61	336.9	12.5

OPTIMIZATION RESULTS

In general, the search of an optimal design that minimizes an unknown objective should not pass by a prior criterion set up. However, in order to compare the behavior of the two algorithms, the optimization problem is reformulated as a goal attainment problem, by which we will impose a design specification on the objective function.

For Both algorithms the Matlab's sequential quadratic programming (SQP) routine is implemented to solve the optimization on the surrogate model. As well as, the use of the same starting point that corresponds to the upper values of the domain denoted by the optimization variables, Table 1, for all specified goals.

Table 5.Radial output space mapping results

E_{Total} **(KJ)**	x_1 **(mm)**	x_2 **(mm)**	x_3 **(mm)**	x_4 **(mm)**	x_5 **(mm)**	x_6 **turns**	T_b **(N.m)**	T_{hs} **(N.m)**	Emf_b **(V)**	Emf_{hs} **(V)**	J **(A.mm^{-2})**	**iter**
1000	150	94.5	9	33.7	50.53	10.77	100	33.33	123.4	256	8.9	7
1100	150	98.7	9.3	40.8	62.03	9.69	100	33.33	74	249.9	8.2	6
1200	150	104.4	8.9	69.6	56.14	10.6	100	33.33	124.8	258	6.8	5
1300	150	106.7	8.8	94.7	49.35	11.14	100	33.33	142.47	260	7.5	5
1400	150	109.49	8.4	106.9	51.6	11.13	100	33.33	150.59	254.7	8.5	4

Here are dressed up the convergence history of the five mappings, for total losses equal to 1300 KJ. These mappings allow us to examine in focus the convergence nature in case of using ROSM and OSM.

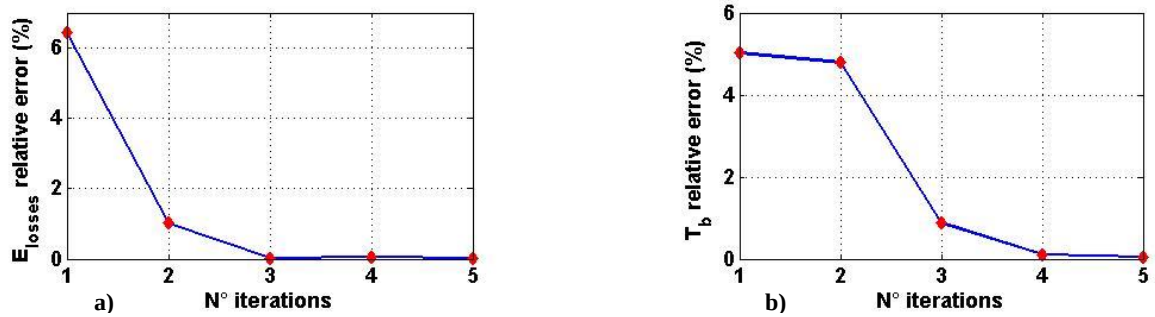

Figure 4.ROSM convergence history for a) the total losses, b) basic torque

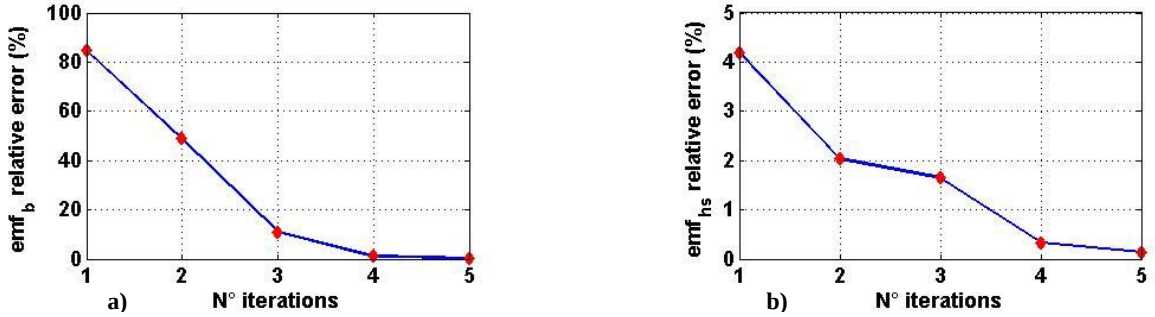

Figure 5.ROSM convergence history for a) basic emf, b) high speed emf

The radial output space mapping history, Fig. 4 and 5, shows a smoothness monotonous convergence towards preset model specifications, as well as convergence values of different output functions Table 5, reflect the rigorous modeling of the surrogate assisted coarse model throughout multilevel optimization phases.

Table 6.Output space mapping results

E_{Total} **(KJ)**	x_1 **(mm)**	x_2 **(mm)**	x_3 **(mm)**	x_4 **(mm)**	x_5 **(mm)**	x_6 **turns**	T_b **(N.m)**	T_{hs} **(N.m)**	Emf_b **(V)**	Emf_{hs} **(V)**	J **(A.mm^{-2})**	**iter**
1000	150	94.5	9	35.7	43.8	11.4	100	33.33	129.4	259	9	7
1100	150	99	9.26	56	38.2	11.8	98.6	33.33	83.3	254	7.29	6
1200	150	104.5	8.9	64.3	51.9	10.19	93.7	33.33	63.4	241	7.13	6
1300	150	102.7	8.79	98.4	43.23	11	92.69	33.33	60.2	245.9	8.02	6
1400	150	109.56	8.4	107.2	51.54	11.15	100	33.33	150.6	255	8.5	4

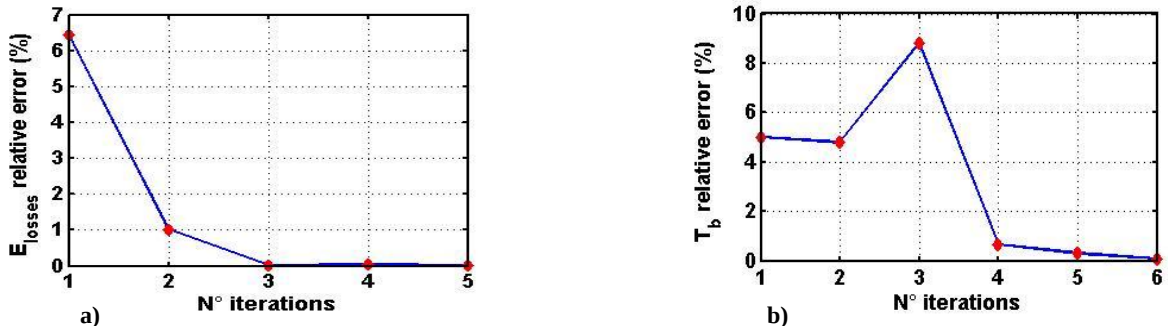

Figure 6.OSM convergence history for a) the total losses, b) basic Torque

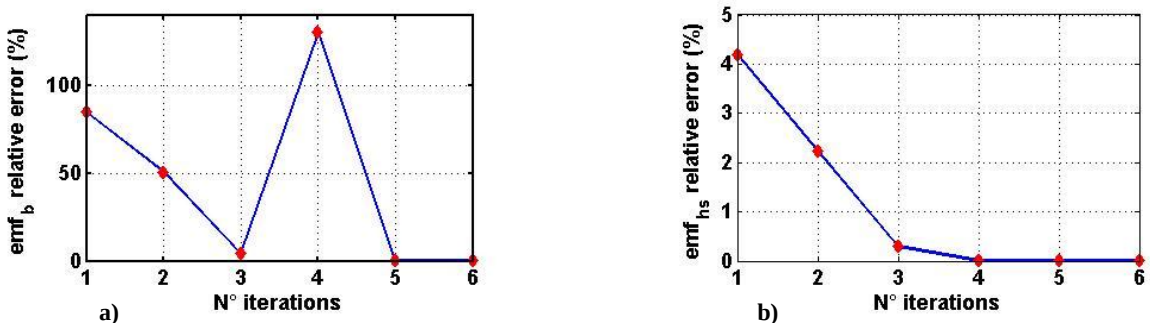

Figure 7.OSM convergence history for a) basic Emf, b) high speed Emf

While, in this case of large discrepancy, alignment of the two models by use of Output Space Mapping may prove to be unsuitable to solve this type of problem. The coupling between basic torque and electromotive forces at basic speed, and the noisy relation between coarse and fine model, can act as primary cause of the noisy, none monotonous convergence reflected by Fig. 6 and 7. As well as, the incapacity of this method to rigorously converge is shown in Table 6.

CONCLUSIONS

The use of a new variant of Output Mapping is proposed in the electromagnetic field in order to increase final robustness of optimal design while using an approximated model, through the progressive construction of a Radial Basis Surrogate model on the bulk of the coarse model. This additive technique from a simple implementation and its efficacious convergence compared to commonly used Output Space Mapping in case of large or non linear misalignment between the two considered fine and coarse model.

The use of these methods can be beneficial in case of standard optimization process, if one considered mapping the output functions that are essentially affected by model's accuracy, as for example magnetic field, forces, torque, while setting as objectives that are not influenced, like total mass, or manufacturing cost.

REFERENCES

[1] J.W. Bandler, Q.S. Cheng, S.A.Dakroury, A.S. Mohamed, M.H.Bakr, K. Madsen, J.Sondergaard.Space mapping: the state of the art, Microwave Theory and Techniques, IEEE Transactions on, vol.52, 2004, no.1, pp. 337- 361.

[2] J.W. Bandler, R.M. Biernacki, C. Shao Hua, P.A. Grobelny, R.H. Hemmers. Space mapping technique for electromagnetic optimization. Microwave Theory and Techniques, IEEE Transactions on, vol.42, 1994, no.12, pp.2536-2544.

[3] C. Hong-Soon, K. Dong-Hun, P. Il-Han, H. Song-Yop. A new design technique of magnetic systems using space mapping algorithm. Magnetics, IEEE Transactions on, 2001, vol.37, no.5, pp.3627-3630.

[4] T.V. Tran, S. Brisset, D. Echeverria, D. Lahaye, P. Brochet. Space-Mapping techniques applied to Optimization of a Safety Isolating Transformer. ISEF, 2007.

[5] S. Vivier, D.Lemoine, G. Friedrich. Fast optimization of a linear actuator by space mapping using unique finite-element model. Industry Applications, IEEE Transactions on, vol.47, 2011, no.5, pp.2059-2065.

[6] R. Ben Ayed, J. Gong,S. Brisset, F. Gillon, P. Brochet. Three-level output space mapping strategy for electromagnetic design optimization. Magnetics, IEEE Transactions on, vol.48, 2012, no.2, pp.671-674.

[7] S. Koziel, J.W. Bandler. Coarse models for efficient space mapping optimization of microwave structures. Microwaves, Antennas & Propagation, IET, vol.4, 2010, no.4, pp.453-465.

[8] J.E. Dennis. A Summary of the Danish Technical University. November 2000 Workshop. Dept. Computational and Applied Mathematics, Rice University, Houston, Texas, 2000.

[9] L. Encica, J. Paulides, E. Lomonova. Space-mapping optimization in electromechanics: an overview of algorithms and applications. COMPEL: The International Journal for Computation and Mathematics in Electrical and Electronic Engineering, Vol. 28, 2009, pp.1216 – 1226.

[10] T. Simpson, J. Poplinski, P. N. Koch, and J. Allen. Metamodels for computer-based engineering design: Survey and recommendations. Engineering with Computers, vol. 17, 2001, pp. 129–150.

[11] Mark J. Orr. Introduction to radial basis function networks. *Technical report*, 1996.

[12] G.M. Laslett. Kriging and splines: An empirical comparison of their predictive performance in some applications. Journal of the American Statistical Association, Vol. 89, 1994, no. 426, pp. 391-400.

[13] M.H.Bakr, J.W.Bandler, M.A.Ismail, J.E.Rayas-Sanchez, Z. Qi-Jun. Neural space-mapping optimization for EM-based design. Microwave Theory and Techniques, IEEE Transactions on, vol.48, 2000, no.12, pp.2307-2315.

[14] E. Davis, M.Ierapetritou. A kriging method for the solution of nonlinear programs with black-box functions. AIChE Journal, Vol. 53, No.8, 2007, pp.2001-2012.

[15] S.Koziel, J.W.Bandler, K. Madsen. Space mapping with adaptive response correction for microwave design optimization. Microwave Theory and Techniques, IEEE Transactions on, vol.57, 2009, no.2, pp.478-486.

[16] S.Koziel, J.W.Bandler. Modeling of microwave devices with space mapping and radial basis functions. International journal of numerical modelling: electronic networks, devices and fields, vol.21, 2008, pp. 1099-1204.

[17] B. Baxter. *The interpolation theory of radial basis functions*. Cambridge University, 1992.

[18] G.Krebs, E.deCecco, C.Marchand. Design approach of an axial flux motor for electrica lpowertrain vehicle. ICEM 2012, 02-05 septembre 2012.

[19] G.Bertotti. General properties of power losses in soft ferromagnetic materials. Magnetics, IEEE Transactions on, vol.24, 1988, no.1, pp.621-630.

[20] E. Hoang. *Etude, modélisation et mesure des pertes magnétiques dans les moteurs à réluctance variable à double saillance*.ENS de Cachan, 1995.

[21] H. Polinder,M.J. Hoeijmakers. Eddy-current losses in the segmented surface-mounted magnets of a PM machine. Electric Power Applications, IEEE Proceedingsvol.146, 1999, no.3, pp.261-266.